Magnetic gap in Slater insulator α'-NaV_2O_5

2008 J. Phys.: Condens. Matter 20 155203

(http://iopscience.iop.org/0953-8984/20/15/155203)

J. Phys.: Condens. Matter **20** (2008) 155203 (10pp) doi:10.1088/0953-8984/20/15/155203

Magnetic gap in Slater insulator α'-NaV_2O_5

Xing Ming[1], Hou-Gang Fan[1,2], Zu-Fei Huang[1,3], Fang Hu[1], Chun-Zhong Wang[1] and Gang Chen[1,4]

[1] Department of Materials Science, College of Materials Science and Engineering, Jilin University, Changchun 130012, People's Republic of China
[2] College of Physics, Jilin Normal University, Siping 136000, People's Republic of China
[3] College of Physics, Jilin University, Changchun 130012, People's Republic of China

E-mail: gchen@jlu.edu.cn

Received 30 October 2007, in final form 15 February 2008
Published 25 March 2008
Online at stacks.iop.org/JPhysCM/20/155203

Abstract

The electronic structure of room-temperature (RT) phase α'-NaV_2O_5 has been investigated by fully self-consistent first-principles calculations based on density functional theory (DFT). For the crystallographic unit cell, a nonmagnetic (NM) metallic solution is obtained by spin-restricted generalized gradient approximation (GGA) calculations, whereas a ferromagnetic (FM) insulating solution is successfully simulated within the spin-polarized GGA. An insulating antiferromagnetic (AFM) state with lower energy is obtained for the $1 \times 2 \times 1$ crystallographic supercell. The magnetic $S = 1/2$ electrons are fully spin-polarized and delocalized on the V–O–V molecular orbitals (along the rung), where the net spin magnetic moments amount to 0.96 μ_B on the V–O–V rungs of the ladder derived from Mulliken population analysis. The intra-rung vanadium d_{xy} orbitals form the bonding–antibonding orbitals split by inter-orbital interactions. It is not the on-site Coulomb interaction, but the AFM spin exchange couplings that lead to the half-filled bonding orbitals splitting and forming a magnetic insulating gap. The present spin-polarized DFT calculations reveal that α'-NaV_2O_5 (RT) is a Slater insulator. The calculated electronic structure explains the controversial topics of the absorption peak in the optical spectra and the energy loss peak in the resonant inelastic x-ray scattering (RIXS).

(Some figures in this article are in colour only in the electronic version)

1. Introduction

Since 1996, the quasi one-dimensional compound α'-NaV_2O_5 has been widely investigated both experimentally and theoretically because of its spin-Peierls (SP) behavior [1]. Its room-temperature (RT) phase, α'-NaV_2O_5 (RT), was first characterized with a non-centrosymmetric structure (P_{21mn} space group) based on x-ray diffraction (XRD) measurements by Carpy and Galy [2]. They suggested that α'-NaV_2O_5 (RT) consisted of magnetic V^{4+} ions ($3d^1$, $S = 1/2$) chains isolated by nonmagnetic V^{5+} ions ($3d^0$, $S = 0$) chains. There are two inequivalent V sites and two distinct nominal charge states based on their XRD work. However, modern single-crystal XRD crystallographic structure studies [3, 4] indicate that α'-NaV_2O_5 (RT) should have a centrosymmetric structure with space group P_{mmn}. This symmetry allows the unique V site and the nominal valence state of V ions to be assigned to an equivalent valence of +4.5. This disordered mixed valence state of V ions [3, 4] is in contrast to the charge ordering pattern [2], but it has been confirmed by a series of experiments such as nuclear magnetic resonance (NMR) [5], Raman/IR scattering spectra [6, 7] and inelastic neutron scattering experiments [8, 9]. The centrosymmetric P_{mmn} structure [3, 4] suggested that α'-NaV_2O_5 (RT) can be viewed as a two-leg ladder in the ab plane, whose legs run along the crystallographic b axis and rungs are oriented along the a direction, that is, α'-NaV_2O_5 (RT) is a quarter-filled ladder compound [4] with only one electron located on the V–O–V rung shared by two V sites.

[4] Author to whom any correspondence should be addressed.

Magnetic behavior of α'-NaV_2O_5 (RT) can be described by a one-dimensional $S = 1/2$ antiferromagnetic (AFM) Heisenberg model, since the spin magnetic susceptibility fits well to the Bonner–Fisher curve [10] above 34 K. The rapid drop of the magnetic susceptibility below 34 K (T_c) was first assigned to a SP transition with a dimerized spin singlet by Isobe and Ueda [1]. The opening of a spin gap is accompanied not only by lattice distortion but also by charge ordering. Fischer *et al* [11] confirmed the spin gap and charge ordering behaviors by light scattering. Fujii *et al* [8] found a superstructure reflection in a single-crystal x-ray scattering experiment and demonstrated spin gap formation by inelastic neutron scattering from a powder sample below the SP transition temperature T_c. They stated that the unit cell doubled both along the a and b axes, but quadrupled along the c axis [8]. Ohama *et al* [5] reported that two inequivalent sets of V sites appeared and were assigned to V^{4+} and V^{5+} states below T_c in the NMR spectra, which strongly suggested the occurrence of charge ordering. However, the low-temperature (LT) structure of α'-NaV_2O_5 (LT) and its charge ordering pattern have been a controversial topic so far. Lüdecke *et al* [12] determined the LT superstructure to be an acentric orthorhombic F_{mm2} on the $2a \times 2b \times 4c$ supercell by synchrotron radiation x-ray diffraction. De Boer *et al* [13] have also succeeded in analyzing the structure below T_c as the space group F_{mm2} with three independent V sites. At the same time, Konstantinović *et al* [6] argued that α'-NaV_2O_5 (LT) should have a symmetry of the $P_{2/b}$ (or $B_{2/b}$—four layers) space group on the basis of symmetry selection rules and Raman scattering spectra. Then Sawa *et al* [14] proposed a monoclinic space group A_{112} for the LT phase. There are several models for the charge ordering phase of α'-NaV_2O_5 (LT), among which the *zig-zag* charge ordering model is widely accepted. The *zig-zag* model is in agreement with NMR [5], electron-paramagnetic resonance (EPR) [15] and x-ray anomalous scattering studies [16]. A high-resolution, highly sensitive synchrotron radiation XRD experiment [17] indicated that the true LT superlattice of α'-NaV_2O_5 should be an F-centered orthorhombic $2a \times 2b \times 4c$ supercell with a stacking disordered *zig-zag* charge ordering. Recently, Ohwada *et al* [18] successfully identified the charge ordering pattern of the LT phase with two types of monoclinically split single domains by applying resonant x-ray scattering (RXS).

Though lots of experiments provide proof in favor of identifying α'-NaV_2O_5 as a SP system, there are several characteristics distinctly deviating from ordinary SP behavior. A comparison of elastic constants and magnetic field effects on the transition temperature with the behavior of the well known inorganic SP compound $CuGeO_3$ has revealed some differences [19]. Vasil'ev *et al* [20] attributed the reason for the anomalous thermal conductivity observed at the phase transition in α'-NaV_2O_5 to a more complicated nature than in $CuGeO_3$. Specific heat measurements [21] indicated that the phase transition in α'-NaV_2O_5 and its behavior in high magnetic fields is incompatible with the notion of being a standard SP transition. The anomalies of the dielectric and magnetic susceptibility in the microwave and far-infrared frequency range indicated that the nature of the spin gap opening in α'-NaV_2O_5 was different from that of $CuGeO_3$ [22]. Based on a combination of heat capacity, electrical resistance and high-temperature electron spin resonance (ESR) experimental observations, Hemberger *et al* [23] concluded that the phase transition in α'-NaV_2O_5 cannot be explained by a SP transition alone. Therefore, it seems that the phase behavior of α'-NaV_2O_5 is so complicated that it cannot only be described with a pure SP model.

RT phase α'-NaV_2O_5 has been intensively investigated theoretically by *ab initio* calculations based on density functional theory (DFT) because of its fascinating characteristics and exotic properties. Smolinski *et al* [4] calculated the energy bands of α'-NaV_2O_5 (RT) within the full-potential linearized augmented plane wave (FP-LAPW) code WIEN97, a nonmagnetic (NM) metallic solution was obtained, which is in conflict with the experimental insulating behavior [23]. They proposed that α'-NaV_2O_5 (RT) with P_{mmn} space group should be a quarter-filled ladder compound with the spins carried by V–O–V molecular orbitals on the ladder rungs [4]. Wu and Zheng [24] investigated the electronic structure of α'-NaV_2O_5 by means of the linear combination of atomic orbital (LCAO) band calculations within both the L(S)DA and the LSDA + U formalism. An NM metallic solution was also obtained by means of L(S)DA band structure calculations. Yaresko *et al* [25] used the tight-binding linear muffin-tin orbital (TB-LMTO) methods in the atomic sphere approximation (ASA) to perform band structure calculations for the RT phase α'-NaV_2O_5, in contrast to experimental results, LDA predicted α'-NaV_2O_5 (RT) to be NM metallic. Spin-restricted band structure calculations [26] were also performed within DFT using the full-potential augmented plane waves together with the local orbital (FP-APW + lo) formalism implemented in the WIEN2K code. The researchers performed geometry relaxation and led to small quantitative differences compared with the results reported in [4]. However, they still did not reproduce the experimental insulating behavior [23]. The realistic description of the nature of the insulating behavior in α'-NaV_2O_5 (RT) has been a challenging question, a detailed discussion and uncovering of the essence of the insulated nature in α'-NaV_2O_5 (RT) are still lacking.

In fact, the electronic structure of α'-NaV_2O_5 (RT) has been widely investigated experimentally by means of optical absorption [27], reflectivity [28, 29] as well as resonant inelastic x-ray scattering (RIXS) [30–32]. Dielectric function and optical conductivity were derived from the optical spectra using the Kramers–Kronig relations, in which an absorption peak at about 0.9 eV was observed [7, 33–35]. However, the nature of this absorption peak has been a controversial topic [27–29]. The explanation of a V d–d energy loss peak of about 1.5 eV in RIXS has also been debated intensively [36, 37]. Therefore, a correct and accurate electronic structure analysis may be desirable and can help us to understand these two issues.

Mila *et al* [38] carried out magnetic susceptibility measurements for α'-NaV_2O_5 and found out that α'-NaV_2O_5 (RT) shows a typical behavior of spin-1/2 chains with the nearest neighbor AFM exchange integral J of 529 K, which was in good agreement with the result reported by Isobe and Ueda [1]. On the other hand, an angle-resolved

photoemission spectroscopy (ARPES) study of α'-NaV_2O_5 at room temperature reveals the doubled periodicity along the b axis, indicating the existence of AFM correlations or holon excitations [39]. These experimental results imply that the magnetic unit cell of α'-NaV_2O_5 (RT) is a $1 \times 2 \times 1$ crystallographic supercell. Though there are two formulas per unit cell in the centrosymmetric P_{mmn} structure of the room-temperature phase, one cannot deal with the magnetic interactions especially that along the ladder leg direction, because there is only one V ion on each leg. Besides, Aichhorn *et al* [40] studied the single-particle properties of α'-NaV_2O_5, applying the variational cluster perturbation theory (V-CPT) to extended Hubbard models. They suggested that the doubling of the unit cell was mainly due to short-range spin correlations whereas charge correlations played only a minor role. It seems that thinking over the magnetic unit cell and the AFM interactions along the ladder legs should be key ingredients to correctly describe the hypostasis of the electronic structure in α'-NaV_2O_5 (RT).

In the present work, detailed electronic structure of α'-NaV_2O_5 (RT) is revealed by fully self-consistent first-principles calculations within DFT. Firstly we obtain the same NM metallic solution for the crystallographic unit cell by the spin-restricted generalized gradient approximation (GGA) calculation. Then α'-NaV_2O_5 (RT) has turned out to be already insulating in the hypothetical ferromagnetic (FM) state for the crystallographic unit cell by our spin-polarized GGA calculation. Therefore the physical properties of α'-NaV_2O_5 (RT) are not strongly influenced by the on-site Coulomb interactions and can be described reliably within DFT. Considering the crystal structure based on a $1 \times 2 \times 1$ crystallographic supercell (doubled along b axis), the system relaxes to an AFM insulating state with AFM interactions along the ladder legs. Calculated results indicate the energy of the AFM magnetic unit cell is the lowest among the NM, FM and AFM solutions. Then the AFM state is the ground state of α'-NaV_2O_5 (RT) from the viewpoint of energy. Based on such spin-polarized DFT calculations, a scenario of the electronic structure for α'-NaV_2O_5 (RT) is presented and, in particular, the essence of the insulating nature has been discussed in detail. Finally the AFM electronic structure helps us to resolve the debate about the optical spectra and the RIXS results.

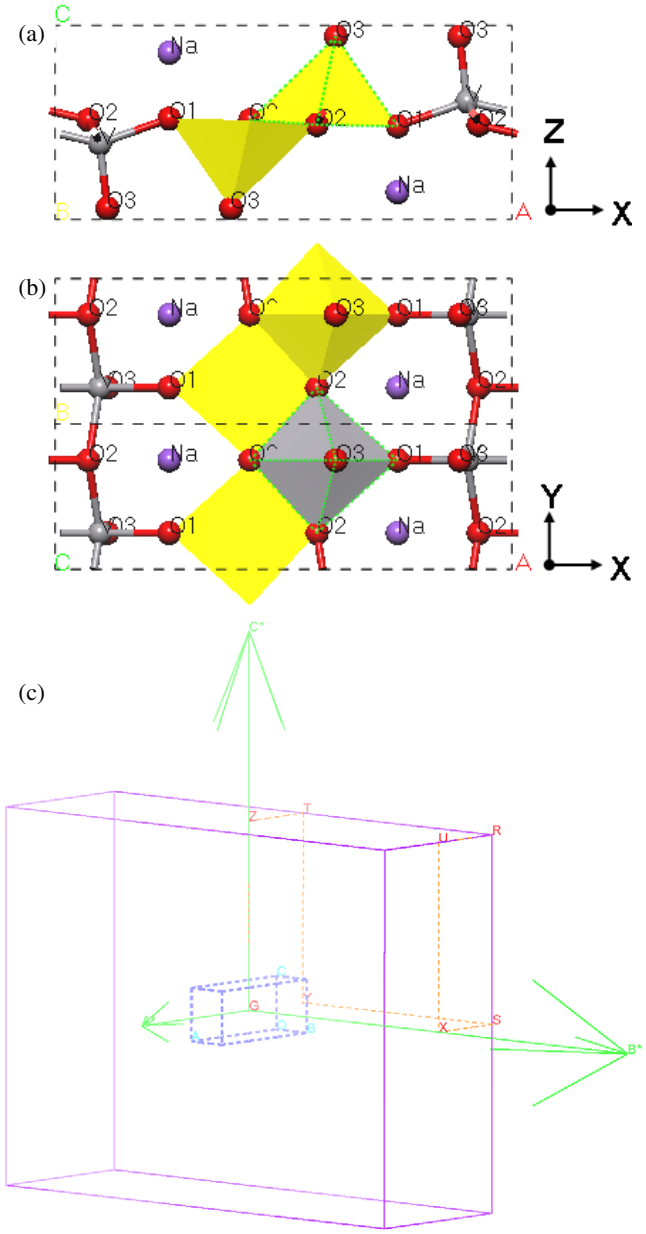

Figure 1. The crystal structure (dashed line rectangle represents a unit cell) of α'-NaV_2O_5 (RT). (a) View along the ladders. (b) View perpendicular to the ladders. (c) The real space unit cell (dashed line hexahedron) and the corresponding reciprocal space Brillouin zone (solid line hexahedron) as well as its highly symmetrical special k points (G, Z, T, Y, S, X, U and R).

2. Computational details

The crystal structure used for calculation is based on the experimental data of α'-NaV_2O_5 (RT) [4]. The lattice parameters are $a = 11.316(4)$ Å, $b = 3.611(1)$ Å, $c = 4.797(2)$ Å and $\alpha = \beta = \gamma = 90°$. The primary crystallographic unit cell contains two formula units with space group P_{mmn}. The crystal structure exhibits double rows of edge-sharing VO_5 pyramids along the b axis with the corner-sharing VO_5 pyramids linked together along the orthorhombic a axis, and shows a two-dimensional characteristic of the ab plane. The Na^+ ions lie between these planes in the interstices of the VO_5 pyramids, as shown in figure 1. There is a unique V and Na site. In addition, there are three O positions denoted as O1, O2 and O3 corresponding to the O ion located on the vertex of the VO_5 pyramid, the O ion of the edge-sharing and the O ion of the corner-sharing. α'-NaV_2O_5 (RT) can be regarded as a two-leg ladder compound in the ab plane. The V and O ions are linked together along the b axis to form the legs of the ladder, while those along the a axis form the rungs of the ladder.

The present calculations are performed within the CASTEP code [41], which employs the DFT plane wave pseudopotential method. Exchange and correlation potentials are treated by GGA (spin-restricted) or spin-polarized GGA (spin-unrestricted) [42]. An ultrasoft pseudopotential [43] is

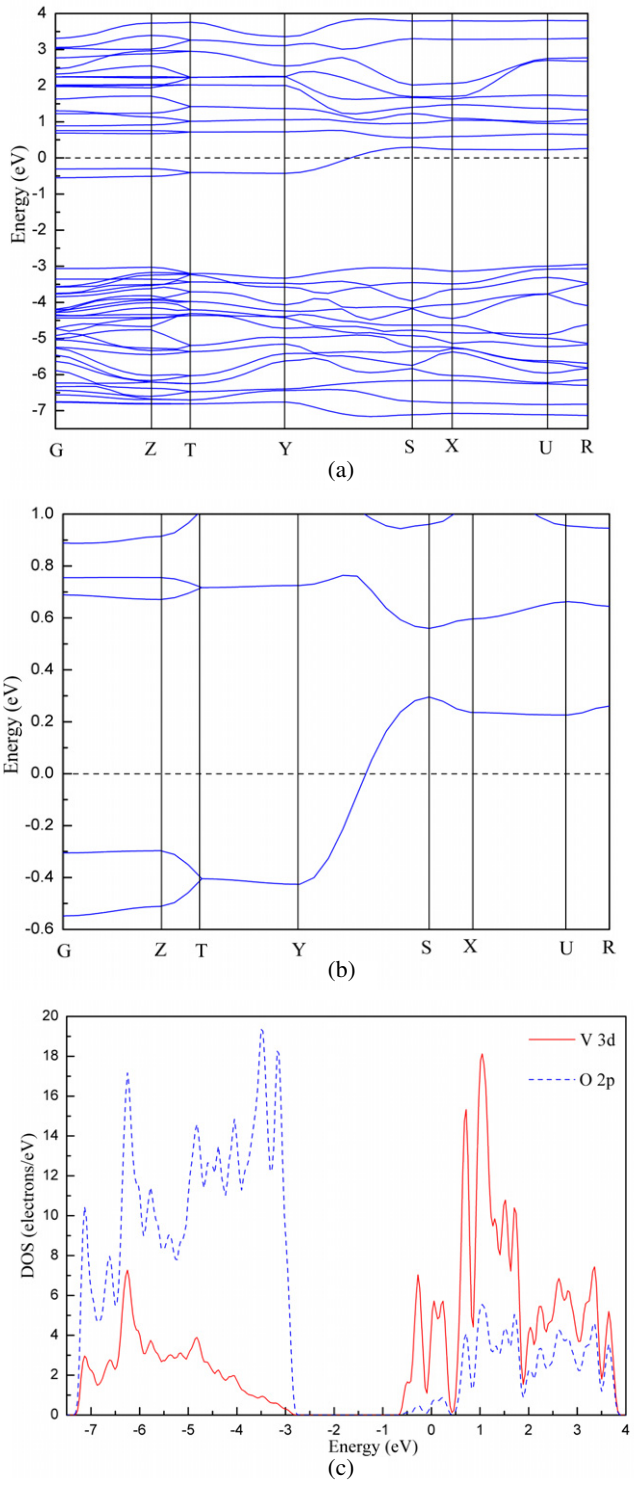

Figure 2. (a) The band structure for the nonmagnetic (NM) state α'-NaV_2O_5 (RT). (b) Enlarged view of the band structure around the Fermi level. (c) The corresponding partial density of states (PDOS) for O 2p orbitals (dashed line) and V 3d orbitals (solid line).

adopted and the GGA proposed by Perdew and Wang [44] is used for the calculations with a plane wave basis set cut-off of 410 eV. Pseudo-atomic calculations are performed for O $2s^2\ 2p^4$, Na $2s^2\ 2p^6\ 3s^1$ and V $3s^2\ 3p^6\ 3d^3\ 4s^2$. The requested k-point spacing is set to 0.04 $Å^{-1}$, which corresponds to a k-point mesh of $2 \times 7 \times 5$ in the irreducible Brillouin zone generated by the Monkhorst–Pack scheme for the unit cell. We first perform fully self-consistent NM-GGA calculations, then adopt the spin-polarized GGA to investigate the electronic and magnetic structure of α'-NaV_2O_5 (RT) for both the $1 \times 1 \times 1$ unit cell and the $1 \times 2 \times 1$ supercell (doubled along b axis).

3. Results and discussion

3.1. NM-GGA calculations for the crystallographic unit cell

The self-consistent spin-restricted (NM) electronic band structure is calculated within the GGA for the crystallographic unit cell. The energy band structure of the NM state along several highly symmetrical directions of the Brillouin zone (BZ) and the corresponding partial density of states (PDOS) for O 2p states as well as V 3d states are plotted in figure 2. The Fermi level, E_F, is set to be 0 eV. The lower valence bands from -7 to -3 eV are mainly formed by O 2p states with partially bonding V 3d hybridization orbitals. The conduction bands extending from 0.6 to 4 eV above E_F are predominantly derived from V 3d states with partial antibonding O 2p hybridization orbitals. There are two nearly degenerate narrow bands spanning the E_F. The present metallic solution is the same as the result reported in [4], where the full-potential linearized augmented plane wave (FP-LAPW) method is used. The pair of energy bands crossing the E_F are predominately attributed to V 3d states, which obviously exhibit quarter-filled characteristics [4]. A closer inspection of the energy band structure near E_F (figure 2(b)) shows that there is another pair of bands separated from the upper conduction bands by a tiny gap of about 0.13 eV. These two pairs of bands are further split across by a gap of about 0.26 eV. In addition, the dispersion along the Y–S direction (i.e. b axis, see the Brillouin zone as shown in figure 1) is very strong, while those in other axes orientations are very weak. It demonstrates the strong one-dimensional character along the b axis of α'-NaV_2O_5, which is in good agreement with the RT ARPES experimental results [39].

The charge density (figure 3) corresponding to the eigenstates of the two pairs of bands around the Fermi level shows that the four bands come mainly from V d_{xy} orbitals, but the upper pair have a partial O p_y component on the rungs, where the x axis is parallel to the rung and y is along the leg. It has been shown in figure 1 that in α'-NaV_2O_5 (RT) a V ion is located inside the deformed VO_5 pyramid which is coordinated with four basal planar O ions and one vertical O ion, so that the degeneracy of the V 3d states is lifted and the V d_{xy} orbitals have the lowest energy according to crystal field theory. V d_{xy} orbitals are separated from the other V 3d orbitals and the 0.13 eV gap is attributed to crystal field splitting. On the other hand, similarly to the H_2^+ case, V d_{xy} orbitals interact with each other on the same rungs, which can form the bonding and antibonding molecular orbitals. Therefore the 0.26 eV gap is assigned to this bonding–antibonding splitting, and the V 3d electrons occupy the bonding orbitals.

Band structure reveals that α'-NaV_2O_5 is metallic, which is inconsistent with the experimentally observed insulating behavior [23, 29, 39]. This metallic solution is the same

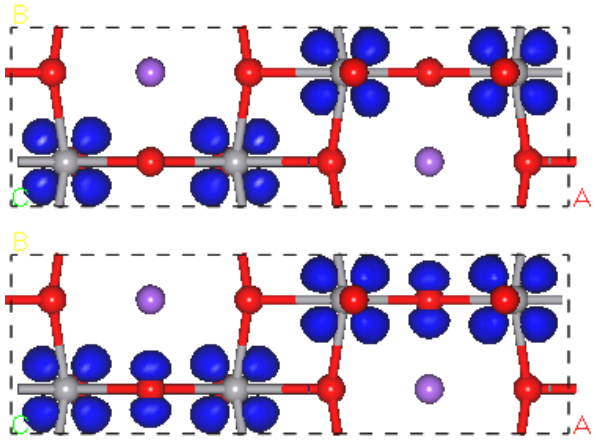

Figure 3. The orbital distribution of the eigenstates corresponding to the two pairs of bands (the top/bottom pattern corresponding to the lower/upper pair) around the Fermi level viewed from the *c* axis (i.e. perpendicular to the *ab* plane).

as other calculated results [4, 24–26]. It was proposed that correlation effects would lead to a charge gap [4]. Wu and Zheng also suggested that the deficiency of the standard DFT methods should be compensated by the U correction to the localized 3d electrons [24]. If this strong-correlation pattern is true, then α'-NaV_2O_5 is a Mott insulator. However, based on the DFT calculations shown in the following subsections, we will show that the insulating behavior is not caused by the charge Coulomb correlation effect, but by the spin magnetic interactions.

3.2. Spin-polarized GGA calculations for the crystallographic unit cell

The metallic solution obtained from the NM-GGA electronic band structure calculations is obviously in contradiction with the experimental observed insulating behavior of α'-NaV_2O_5 (RT). Formally, there is one unpaired electron in each NaV_2O_5 formula and there are two formulas in the unit cell of α'-NaV_2O_5 (RT), so we specify the total net spin as being 2 before performing a spin-polarized GGA calculation to simulate a hypothetical FM state in the unit cell.

The electronic structure of the hypothetical FM state is shown in figure 4, the lower valence bands from -7 to -2.8 eV are almost the same as the NM calculated results. They are separated from the upper pair of valence bands located from about -0.9 eV to E_F by a gap of about 2 eV. The two upper valence bands as well as all the conduction bands are derived predominately from V 3d states hybridized with partial O 2p states. In fact, the characteristics of the present two pairs of *up*-spin subbands around E_F are almost identical to the NM case. A pair of *down*-spin valence bands shifts down relatively to another pair located near the bottom of the conduction bands. An insulating energy gap of only about 0.11 eV arises between the top of *up*-spin valence bands and the bottom of *down*-spin conduction bands located above E_F.

The electronic spin density (the difference between the charge density of *up*-spin and *down*-spin electrons) for the

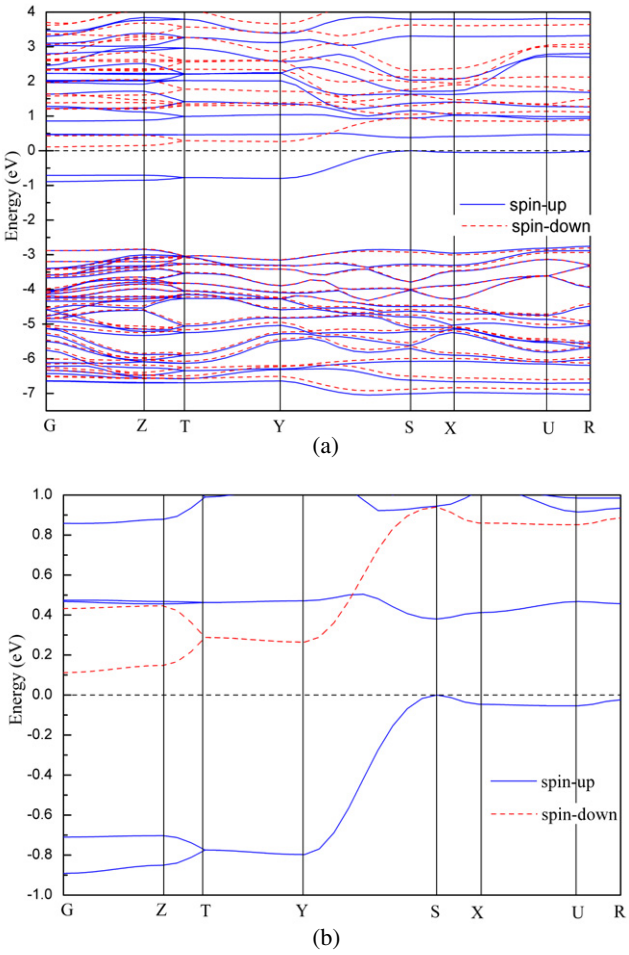

Figure 4. (a) Band structure for the ferromagnetic (FM) solution of α'-NaV_2O_5 (RT). (b) Enlarged view of the band structure around the Fermi level. The solid/dashed lines correspond to the spin-*up/down* subbands.

present FM solution is shown in figure 5, which allows us to visualize the spatial distribution of the magnetic moment in the spin-polarized system. It is clear that the V 3d electrons are fully delocalized on the two sites of the rungs and occupy an orbital with d_{xy} character (where the x axis is parallel to the rung and y is along the leg), while the O sites on the same rungs and the nearest neighbor vertexes carry a minority of opposite spin magnetic moments relative to the V sites. The spin density distribution and the symmetry of the involved d and p orbitals reflect the FM magnetic coupling between V ions via the intervening O ions on the same rungs as well as along the leg direction in the *ab* plane.

By the present spin-polarized GGA calculation, the experimental insulating behavior of α'-NaV_2O_5 (RT) has already been successfully reproduced. The quarter-filled V d_{xy} orbitals are separated from the other V 3d orbitals by VO_5 pyramid crystal field splitting, then what is the cause of the further splitting of the V d_{xy} orbitals? And what causes the insulating gap between the occupied *up*-spin and unoccupied *down*-spin V d_{xy} bands to be induced? Other investigations focused only on the Coulomb correlation effects and considered the U correction to the LDA, but they ignored

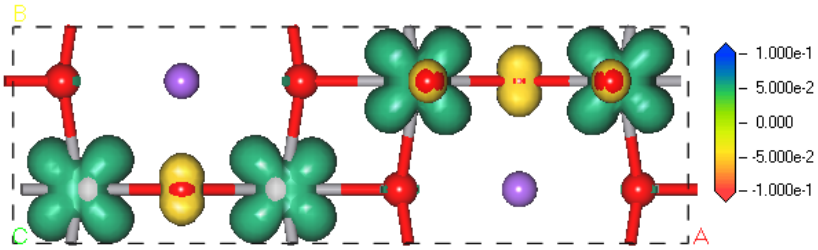

Figure 5. Iso-surface of the electronic spin density (electrons per $Å^3$) for the ferromagnetic (FM) solution in a unit cell viewed from the *c* axis (i.e. perpendicular to the *ab* plane) with an iso-value of 0.05.

the fact that they had also taken into account the AFM interactions along the ladder legs of α'-NaV_2O_5 (RT). We will demonstrate in the following subsections that α'-NaV_2O_5 (RT) cannot be assigned arbitrarily to the strongly correlated system, and the magnetic spin exchange interactions are the sticking points in the understanding of the essence of the electronic structure of α'-NaV_2O_5 (RT). On the contrary, the effect of the on-site Coulomb repulsion interactions indeed play a trivial role in deciding the characteristic of α'-NaV_2O_5 (RT).

3.3. Spin-polarized GGA calculations for the $1 \times 2 \times 1$ *supercell*

The band structure displayed in figure 2(a) exhibits nesting along the T–Y direction near the Fermi level which suggests the instability with respect to the doubled periodicity along the *b* axis [45, 46]. Although the insulating FM solution is consistent with the experimental insulating behavior, α'-NaV_2O_5 (RT) as a one-dimensional spin-1/2 antiferromagnetic (AFM) Heisenberg chain [1, 38] cannot be explained. It has been shown previously that ARPES measurement [39] suggests the existence of doubled periodicity along the crystallographic *b* axis. As mentioned above, there are two formulas per unit cell, but we cannot deal with the complex magnetic interactions especially along the ladder direction because there is only one V atom on each leg in a unit cell (see figure 1(b)). In addition, it has been widely accepted that the magnetic interactions are supposed to take place principally in the *ab* plane [47]. Therefore, we choose such a superstructure with a doubled periodicity along the *b* axis ($1 \times 2 \times 1$ supercell) to perform a fully self-consistent calculation with spin-polarized GGA. Katoh *et al* [46] considered the AF order along the *b* axis and the FM order along the *a* axis beforehand. In the present work, we just fix the net spin to 0 before performing the spin-polarized GGA calculation. We do not assign artificially a special magnetic ordering, but let the CASTEP code automatically relax during the calculation process to search for the lowest energy state in the $1 \times 2 \times 1$ supercell.

The band structure and corresponding total spin density of states (DOS) are displayed in figure 6. Distinguished from the FM solution, the main change in the energy bands is that the *up*-spin and *down*-spin subbands overlap each other. Both states in the DOS are absolutely identical at the same energy, displaying the unique characteristic of the AF ordering. Therefore the system has relaxed to an AFM state in the $1 \times 2 \times 1$ supercell. Similarly to the NM and the FM solutions, the lower part of the valence bands are formed from O 2p states with partial V 3d bonding hybridization orbitals. They are separated by a gap of about 2 eV from the upper valence bands extending from -0.3 eV to the Fermi level. The conduction bands above E_F are derived mainly from V 3d states with partial O 2p antibonding hybridization orbitals. The narrow conduction bands lying around 0.8 eV above E_F are separated by an insulating energy gap of about 0.77 eV (see figure 6(c)) from the top of the valence bands. These bands are split by a gap of about 0.3 eV from the upper conduction bands.

Horsch and Mack [48] have shown that the insulating behavior of α'-NaV_2O_5 (RT) can be reproduced with a charge gap of $2t_\perp$, where $t_\perp$ is the hopping term on the same V–O–V rung. Mapping the DFT bands on the tight-binding model, Smolinski *et al* [4] obtained $t_\perp = 0.38$ eV in α'-NaV_2O_5 (RT). The calculated gap value of 0.77 eV is in good agreement with the result of Smolinski *et al* [4]. The theoretical insulating gap corresponds to the on-rung excitation from V 3d bonding to antibonding orbitals, which is also comparable with the observed 0.8–1 eV absorption peak in the optical conductivity [28, 34, 35] as well as the optical gap measured by Golubchik *et al* [27]. In addition, the calculated charge transfer energy from the O 2p states to V 3d states is approximate 3.3 eV as shown in figure 6(b), which is in accordance with the optical conductivity data and optical absorption spectra of α'-NaV_2O_5 (RT) [27, 28, 34, 35]. Although the gap excitation is d–d type, which is consistent with the ARPES [39] experiment and other theoretical calculations [24], the origin of the gap is not Coulomb correlation effects U, and the nature of the insulating state cannot be assigned to either Mott–Hubbard type [24] or charge transfer type [4]. Though an AFM insulating solution has also been obtained in [46], Katoh *et al* stressed the crystal structure and the symmetry problem and did not discuss the essence of the insulated nature. We will give detailed analysis later on about the nature of the insulating gap (section 3.4) and explanations for the optical properties and RIXS result (section 3.5) based on our calculated electronic structure.

Figure 7 shows the electronic spin density for the present AFM solution. On the one hand, all the V 3d electrons occupy the d_{xy} orbitals; on the other hand, V 3d electrons in the rungs are fully spin-polarized. So far, we have obtained the NM, FM as well as AFM solutions. It should be noted that the V 3d electrons' occupation of the d_{xy} orbitals is actually determined by the crystal field. This orbital ordering is not

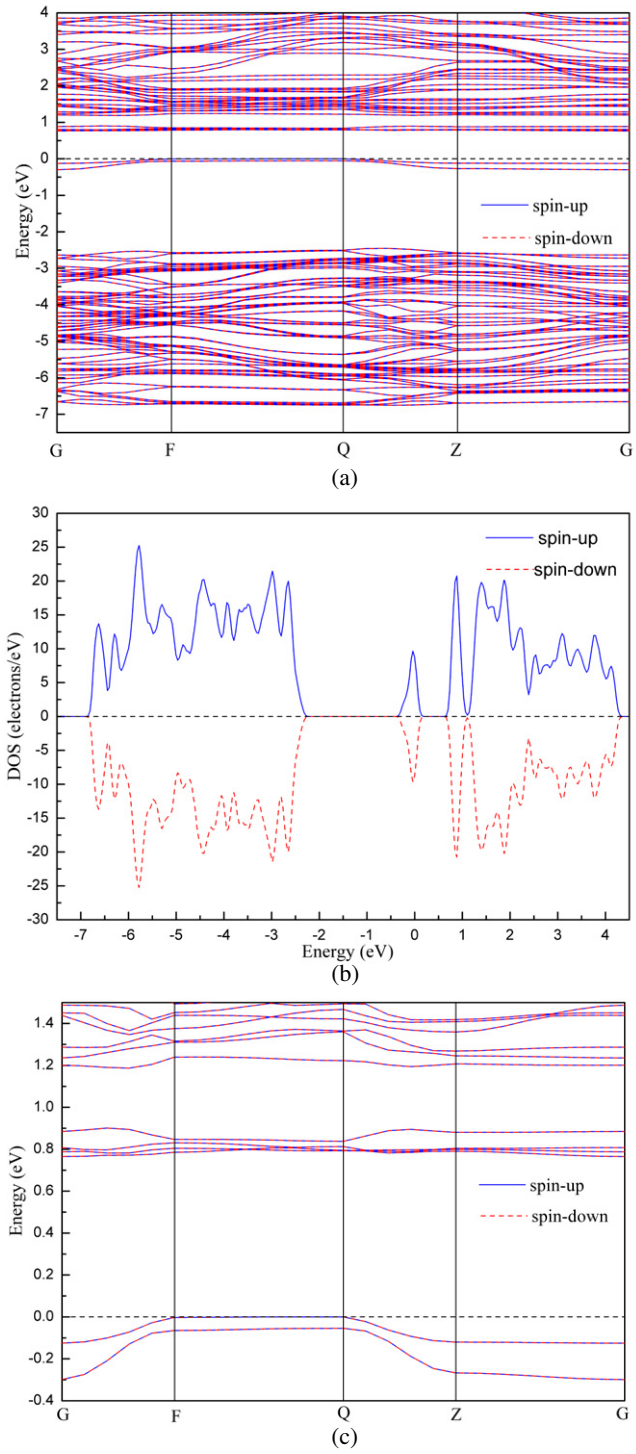

Figure 6. (a) Band structure for the antiferromagnetic (AF) solution and (b) the corresponding total spin density of states (DOS), Spin-*up/down* states are plotted along the positive/negative coordinate; (c) enlarged view of the band structure around the Fermi level. The solid/dashed lines correspond to the spin-*up/down* subbands.

related to the magnetic ordering, which is shown in figures 3, 5 and 7. The on-rung orbital ordering of V sites can lead to a very strong hybridization and exchange coupling effect through the interval O atom, because the lobes of the V d_{xy}

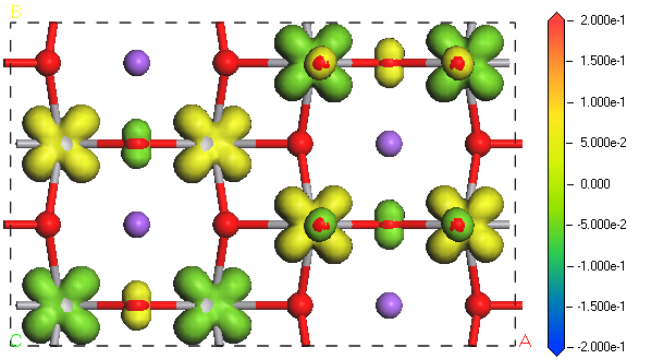

Figure 7. Iso-surface of the electronic spin density (electrons per $Å^3$) for the present AFM solution in the $1 \times 2 \times 1$ supercell viewed from the *c* axis (i.e. perpendicular to the *ab* plane) with an iso-value of 0.05.

orbitals overlap with O p_y orbitals to the utmost extent on the same rung. The local spin magnetic moment at each V site is equal to 0.52 μ_B from Mulliken population analysis ([46] obtained a value of 0.42 μ_B). The intra-ladder spins are antiparallel to each other along the legs and parallel on the same rungs. There are minor local residual spin magnetic moments of about 0.08 μ_B on each rung O sites, and 0.06 μ_B on the vertical O sites, both of which have opposite orientations to the nearest neighbor V sites. In fact, *ab initio* quantum chemical calculations [49] using large configuration interaction (CI) methods on embedded fragments have shown that the $2p_y$ electrons of the bridging O on the rungs present a very strong magnetic character and should be explicitly taken into account while modeling the compound. The O hole character on the rung has been recently confirmed by density-matrix renormalization group (DMRG) methods [50]. If we consider the whole V–O–V rung molecular orbital, V $3d_{xy}$–O $2p_y$–V $3d_{xy}$ orbitals form a pd π type bond on the same rung, and the net spin magnetic moments on each rung is approximately 0.96 μ_B, comparable with an $S = 1/2$ magnetic electron. Since the charge and spin populations on every V site are equal to 1/2, therefore α'-NaV_2O_5 (RT) is called a quarter-filled spin ladder [4]. Hozoi *et al* [51] performed complete active space self-consistent field (CASSCF) calculations on embedded clusters, and propose a rung ground state with V $3d^1_{xy}$–O $2p^1_y$–V $3d^1_{xy}$ character in the RT phase. They suggested the idea of an unpaired electron shared by two V ions instead of the conventional picture of a closed O 2p shell [51]. It is concluded that the magnetic $S = 1/2$ electrons should not only be carried by the V 3d orbitals but delocalized on the V–O–V rungs. The present result is similar to the one-dimensional effective spin system proposed by Horsch and Mack [48], with an effective $S = 1/2$ spin on each rung and AFM coupling along the ladder. The *ab initio* DFT calculated result is also similar to the *ab initio* quantum chemical calculations by Suaud and Lepetit [52], where α'-NaV_2O_5 (RT) is described as a two-dimensional triangular Heisenberg system with an effective AFM coupling along the ladders, whereas there is FM coupling in the other two directions.

3.4. Nature of the insulating state

It has been demonstrated that in the RT phase of α'-NaV_2O_5, the magnetic $S = 1/2$ electrons are delocalized on the V–O–V molecular orbitals, which corresponds to the orbital population 1/2 on every V site (if the spin degeneracy is considered, then the orbital population is 1/4). In such a situation, the on-site Coulomb repulsion interaction is not important [53], instead the inter-site exchange coupling effects should play an important role in determining the transport, optical, thermodynamic as well as magnetic properties of α'-NaV_2O_5 (RT). The insulating gap is induced by magnetic interaction in α'-NaV_2O_5 (RT). According to Korbel *et al* [54], the band gap in α'-NaV_2O_5 (RT) is a magnetic gap. This magnetic gap is formed by both the doubled periodicity in the crystallographic *b* axis and the spin exchange interaction. The metal–insulator transition from paramagnetic ($1 \times 1 \times 1$ cell) to AFM ($1 \times 2 \times 1$ cell) states is a direct consequence of the Brillouin zone folding generated by magnetic ordering [55]. Therefore, α'-NaV_2O_5 (RT) is a Slater insulator [55, 56]. Unlike a Mott insulator in which the spin and charge degrees of freedom are decoupled, a Slater insulator exhibits a coupled spin and charge degrees of freedom [55].

Like Mott transition, Slater transition occurs in the half-filled band [57]. However, α'-NaV_2O_5 (RT) is known as a quarter-filled ($n = 1/2$) compound [4]. Whether or not Slater transition can be used to explain the insulating behavior of α'-NaV_2O_5 (RT) is correlated to whether the band is quarter-filled or half-filled. As mentioned above, the VO_5 pyramids' crystal field leads the five-fold degenerated V 3d orbitals to split-off. The d_{xy} orbitals have the lowest energy, and are separated from the other V 3d orbitals by a gap (refer to figures 2 and 4). The d_{xy} orbitals interact with each other via O p_y orbitals on the same rung, forming the bonding d_{xy} and antibonding d^*_{xy} orbitals. The energy of the bonding orbitals is lower than the antibonding orbitals, and the V 3d electrons only occupy the H_2^+-type bonding d_{xy} orbitals. There are eight V atoms in the $1 \times 2 \times 1$ supercell and four bonding d_{xy} and four antibonding d^*_{xy} orbitals. Considering the spin degree of freedom, each bonding or antibonding orbital is two-fold degenerated. There is only one unpaired electron per formula for α'-NaV_2O_5 (RT), so there are four unpaired 3d electrons in the $1 \times 2 \times 1$ supercell. Due to the gap between the bonding and antibonding orbitals (see figure 8(a)), the eight-fold degenerated bonding d_{xy} spin-orbitals are half-filled. It is the splitting of the V bonding d_{xy} and antibonding d^*_{xy} orbitals that result in half-filled 3d bands. AFM interaction further influences the relative energy of both bonding and antibonding orbitals, namely, the AFM exchange coupling interaction leads to a further splitting of the V d_{xy} bonding and antibonding d^*_{xy} orbitals in half (to aid our understanding, we can refer to the schematic pattern in figure 8): one half of the d_{xy} orbitals (both bonding and antibonding) shifts to a lower energy range whereas the other half shifts to a higher energy region, and the upper half of the bonding d_{xy} orbitals mixes with the lower half of the antibonding d^*_{xy} orbitals. From the band structure of the AFM insulating solution, we can see that the two pairs of valence bands near E_F are primarily vanadium d_{xy} bonding orbitals. Consequently, the four pairs of conduction bands near

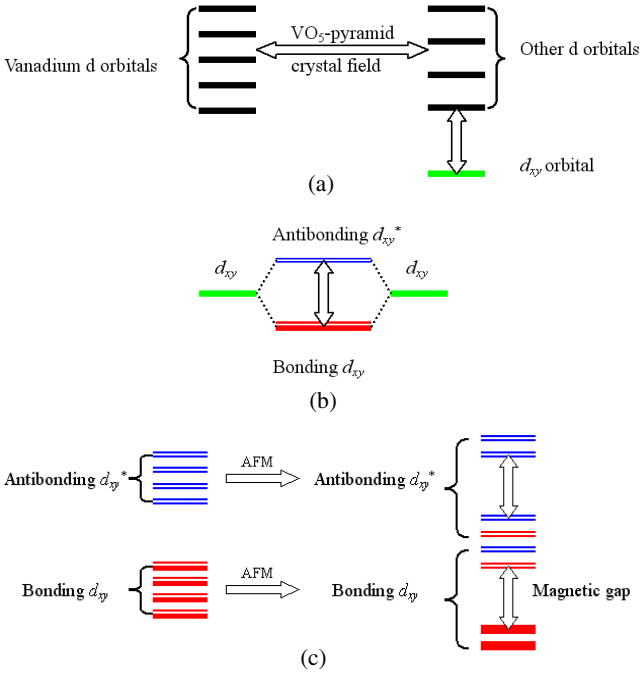

Figure 8. Schematic illustration of vanadium 3d states in α'-NaV_2O_5 (RT). (a) Five-fold degenerated V 3d orbitals are split by the VO_5-pyramid crystal field, the orbital with d_{xy} symmetry has lower energy and is separated from the other orbitals; (b) the hybridizations of the d_{xy} orbitals give rise to a bonding–antibonding splitting; (c) the half-filled bonding d_{xy} spin orbitals are split in half by the AFM interactions along the ladder leg direction, resulting in a magnetic gap.

E_F are made up of the two pairs of vanadium d_{xy} bonding and two pairs of antibonding d^*_{xy} orbitals. Another two pairs of antibonding orbitals shift to the higher energy region and hybridize with other vanadium 3d orbitals, which annihilate the crystal field energy gap between the V d_{xy} orbitals and the other 3d orbitals. This change is reflected by the DOS plots shown in figure 6(b) (we should be aware that the tail of the DOS at E_F is attributed to the Gaussian smearing), in which the intensity of the DOS for the valence band near E_F is about half of the first conduction band.

3.5. Optical spectra and RIXS

Optical studies of α'-NaV_2O_5 have been carried out to study the electronic structure experimentally. Several different interpretations had been put forward for the 0.9 eV absorption peak in the optical spectra, such as transitions between bonding and antibonding V d_{xy} orbitals [4, 7, 28, 33, 35], transitions between V 3d orbitals with different symmetry [29] as well as on-site transitions between V 3d orbitals owing to the crystal field splitting [27]. We suggest that the magnetic insulating gap of the AFM solution corresponds to this optical gap, which is for on-rung transitions from vanadium bonding d_{xy} orbitals to antibonding d^*_{xy} orbitals, as shown in figure 6. Consistency between our calculated 0.77 eV and observed 0.9 eV is satisfied.

RIXS can directly probe the d–d transition between the occupied and unoccupied states [30, 32]. In the RIXS spectra

of α'-NaV_2O_5 (RT), a sharp energy loss feature at about 1.5 eV was observed. However, the interpretations for this d–d peak have been debated intensively [30, 32, 36, 37]. Zhang *et al* [30, 32, 37] pointed out that the d–d peak arises from excitation between the lower and upper Hubbard hands. Other studies [36] suggested that the d–d peak arises from the excitation from filled d_{xy} orbitals into unoccupied d_{xz} and d_{yz} orbitals. Angle-resolved RIXS (ARRIXS) was used to investigate the origin of the d–d peak [32], which revealed that the d–d transition involves both the unoccupied d_{xy} and $d_{xz/yz}$ orbitals. ARRIXS [32] indicated that energy losses of the d–d transitions for d_{xy}–d_{xy} and d_{xy}–$d_{xz/yz}$ were about 1.5 eV and 2 eV, respectively. From the AFM insulating solution (refer to figures 6 and 8), we know that the lowest energy loss peak in the RIXS spectra should be attributed to the transitions from occupied bonding d_{xy} orbitals (valence band) to unoccupied bonding d_{xy} orbitals (the first conduction band), and higher energy loss should be attributed to the transition from bonding d_{xy} orbitals (valence band) to unoccupied $d_{xz/yz}$ orbitals (the second conduction band). The electronic structure of the AFM insulating solution is consistent with the ARRIXS experiment.

4. Summary and conclusions

The present research has studied the electronic structure of α'-NaV_2O_5 (RT) with first-principles band structure calculations by both GGA and spin-polarized GGA. The NM metallic solutions for α'-NaV_2O_5 (RT) within a crystallographic unit cell are obtained, which are the same as the results calculated with other methods but in contradiction to the experimentally observed insulating behavior. The room-temperature phase of α'-NaV_2O_5 relaxed to the FM state in a unit cell and AFM state in the $1 \times 2 \times 1$ supercell, respectively. The total energy is higher in NM metallic state than that of the FM and AFM insulating state by 34.8 meV per formula unit(/f.u.) and 83.8 meV/f.u., respectively. From the viewpoint of the energy, the NM metallic state is unstable relative to the magnetic ordering insulating state, the AFM state is the ground state of α'-NaV_2O_5 (RT). AFM correlations along the ladder leg direction offer a good interpretation for the doubled periodicity along the b axis in the ARPES study and the spin magnetic susceptibility behavior of the one-dimensional $S = 1/2$ Heisenberg AFM chain in α'-NaV_2O_5 (RT). The magnetic $S = 1/2$ electrons are delocalized on the ladder rungs of V–O–V molecular orbitals, the intra-rung vanadium d_{xy} orbitals form the bonding–antibonding orbitals, splitting via inter-orbital interaction. It is not the on-site Coulomb interaction, but the AFM spin exchange couplings that lead to the half-filled bonding orbitals splitting and forming a magnetic insulating gap. Therefore, α'-NaV_2O_5 (RT) is a Slater insulator. The calculated electronic structure explains well the absorption peak in the optical spectra and the energy loss peak in RIXS.

Acknowledgments

This work was sponsored by both the Chinese National Science Foundation under Grant No. 50672031 and the Program for Changjiang Scholars and the Innovative Research Team in the University under Grant No. IRT0625. This work was also partially supported by the Scientific and Technological Research and Development program of Jilin Province, China under Grant No. 20060511.

References

[1] Isobe M and Ueda Y 1996 *J. Phys. Soc. Japan* **65** 1178
[2] Carpy A, Casalot A, Pouchard M, Galy J and Hagenmuller P 1972 *J. Solid State Chem.* **5** 229
Carpy A and Galy J 1975 *Acta Crystallogr.* B **31** 1481
[3] Meetsma A, de Boer J L, Damascelli A, Jegoudez J, Revcolevschi A and Palstra T T M 1998 *Acta Crystallogr.* C **54** 1558
von Schnering H G, Grin Y, Kaupp M, Somer M, Kremer R K, Jepsen O, Chatterji T and Weiden M 1998 *Z. Kristallogr.* **213** 246
Chatterji T, Liß K D, McIntyre G J, Weiden M, Hauptmann R and Geibel C 1998 *Solid State Commun.* **108** 23
[4] Smolinski H, Gros C, Weber W, Peuchert U, Roth G, Weiden M and Geibel C 1998 *Phys. Rev. Lett.* **80** 5164
[5] Ohama T, Yasuoka H, Isobe M and Ueda Y 1999 *Phys. Rev.* B **59** 3299
[6] Konstantinović M J, Popović Z V, Vasil'ev A N, Isobe M and Ueda Y 1999 *Solid State Commun.* **112** 397
[7] Damascelli A, Presura C, van der Marel D, Jegoudez J and Revcolevschi A 2000 *Phys. Rev.* B **61** 2535
[8] Fujii Y, Nakao H, Yosihama T, Nishi M, Nakajima K, Kakurai K, Isobe M, Ueda Y and Sawa H 1997 *J. Phys. Soc. Japan* **66** 326
[9] Yosihama T, Nishi M, Nakajima K, Kakurai K, Fujii Y, Isobe M, Kagami C and Ueda Y 1998 *J. Phys. Soc. Japan* **67** 744
[10] Bonner J C and Fisher M E 1964 *Phys. Rev.* **135** A640
[11] Fischer M, Lemmens P, Els G, Güntherodt G, Sherman E Ya, Morré E, Geibel C and Steglich F 1999 *Phys. Rev.* B **60** 7284
[12] Lüdecke J, Jobst A, van Smaalen S, Morré E, Geibel C and Krane H G 1999 *Phys. Rev. Lett.* **82** 3633
[13] de Boer J L, Meetsma A, Baas J and Palstra T T M 2000 *Phys. Rev. Lett.* **84** 3962
[14] Sawa H, Ninomiya E, Ohama T, Nakao H, Ohwada K, Murakami Y, Fujii Y, Noda Y, Isobe M and Ueda Y 2002 *J. Phys. Soc. Japan* **71** 385
[15] Lohmann M, Krug von Nidda H A, Eremin M V, Loidl A, Obermeier G and Horn S 2000 *Phys. Rev. Lett.* **85** 1742
[16] Nakao H, Ohwada K, Takesue N, Fujii Y, Isobe M, Ueda Y, Zimmermann M V, Hill J P, Gibbs D, Woicik J C, Koyama I and Murakami Y 2000 *Phys. Rev. Lett.* **85** 4349
[17] van Smaalen S, Daniels P, Palatinus L and Kremer R K 2002 *Phys. Rev.* B **65** R060101
[18] Ohwada K, Fujii Y, Katsuki Y, Muraoka J, Nakao H, Murakami Y, Sawa H, Ninomiya E, Isobe M and Ueda Y 2005 *Phys. Rev. Lett.* **94** 106401
[19] Fertey P, Poirier M, Castonguay M, Jegoudez J and Revcolevschi A 1998 *Phys. Rev.* B **57** 13698
[20] Vasil'ev A N, Pryadun V V, Khomskii D I, Dhalenne G, Revcolevschi A, Isobe M and Ueda Y 1998 *Phys. Rev. Lett.* **81** 1949
[21] Köppen M, Pankert D, Hauptmann R, Lang M, Weiden M, Geibel C and Steglich F 1998 *Phys. Rev.* B **57** 8466
Johnston D C, Kremer R K, Troyer M, Wang X, Klümper A, Bud'ko S L, Panchula A F and Canfield P C 2000 *Phys. Rev.* B **61** 9558
Schnelle W, Grin Y and Kremer R K 1999 *Phys. Rev.* B **59** 73
[22] Smirnov A I, Popova M N, Sushkov A B, Golubchik S A, Khomskii D I, Mostovoy M V, Vasil'ev A N, Isobe M and Ueda Y 1999 *Phys. Rev.* B **59** 14546

[23] Hemberger J, Lohmann M, Nicklas M, Loidl A, Klemm M, Obermeier G and Horn S 1998 *Europhys. Lett.* **42** 661
[24] Wu H and Zheng Q Q 1999 *Phys. Rev.* B **59** 15027
[25] Yaresko A N, Antonov V N, Eschrig H, Thalmeier P and Fulde P 2000 *Phys. Rev.* B **62** 15538
[26] Spitaler J, Sherman E Y, Evertz H G and Ambrosch-Draxl C 2004 *Phys. Rev.* B **70** 125107
[27] Golubchik S A, Isobe M, Ivlev A N, Mavrin B N, Popova M N, Sushkov A B, Ueda Y and Vasil'ev A N 1999 *J. Phys. Soc. Japan* **66** 4042
Golubchik S A, Isobe M, Ivlev A N, Mavrin B N, Popova M N, Sushkov A B, Ueda Y and Vasil'ev A N 1999 *J. Phys. Soc. Japan* **68** 318 (erratum)
[28] Damascelli A, van der Marel D, Grüninger M, Presura C, Palstra T T M, Jegoudez J and Revcolevschi A 1998 *Phys. Rev. Lett.* **81** 918
[29] Long V C, Zhu Z, Musfeldt J L, Wei X, Koo H J, Whangbo M H, Jegoudez J and Revcolevschi A 1999 *Phys. Rev.* B **60** 15721
[30] Zhang G P, Callcott T A, Woods G T, Lin L, Sales B, Mandrus D and He J 2002 *Phys. Rev. Lett.* **88** 077401
Zhang G P, Callcott T A, Woods G T, Lin L, Sales B, Mandrus D and He J 2002 *Phys. Rev. Lett.* **88** 189902 (erratum)
[31] Zhang G P, Woods G T, Shirley E L, Callcott T A, Lin L, Chang G S, Sales B C, Mandrus D and He J 2002 *Phys. Rev.* B **65** 165107
Woods G T, Zhang G P, Callcott T A, Lin L, Chang G S, Sales B C, Mandrus D and He J 2002 *Phys. Rev.* B **65** 165108
[32] Zhang G P and Callcott T A 2006 *Phys. Rev.* B **73** 125102
[33] Presura C, van der Marel D, Dischner M, Geibel C and Kremer R K 2000 *Phys. Rev.* B **62** 16522
[34] Presura C, van der Marel D, Damascelli A and Kremer R K 2000 *Phys. Rev.* B **61** 15762
[35] Konstantinović M J, Popović Z V, Moshchalkov V V, Presura C, Gajić R, Isobe M and Ueda Y 2002 *Phys. Rev.* B **65** 245103
[36] Duda L C, Schmitt T, Nordgren J, Kuiper P, Dhalenne G and Revcolevschi A 2004 *Phys. Rev. Lett.* **93** 169701
van Veenendaal M and Fedro A J 2004 *Phys. Rev. Lett.* **92** 219701
[37] Zhang G P, Callcott T A, Woods G T, Lin L, Sales B C, Mandrus D and He J 2004 *Phys. Rev. Lett.* **93** 169702
Zhang G P, Callcott T A, Woods G T, Lin L, Sales B C, Mandrus D and He J 2004 *Phys. Rev. Lett.* **92** 219702
[38] Mila F, Millet P and Bonvoisin J 1996 *Phys. Rev.* B **54** 11925
[39] Kobayashi K, Mizokawa T, Fujimori A, Isobe M and Ueda Y 1998 *Phys. Rev. Lett.* **80** 3121
[40] Aichhorn M, Sherman E Y and Evertz H G 2005 *Phys. Rev.* B **72** 155110
[41] Segall M D, Lindan P J D, Probert M J, Pickard C J, Hasnip P J, Clark S J and Payne M C 2002 *J. Phys.: Condens. Matter* **14** 2717
[42] Perdew J P, Burke K and Ernzerhof M 1996 *Phys. Rev. Lett.* **77** 3865
[43] Vanderbilt D 1990 *Phys. Rev.* B **41** 7892
[44] Perdew J P and Yue W 1986 *Phys. Rev.* B **33** 8800
[45] Popović Z S and Vukajlović F R 2002 *J. Phys. Soc. Japan* **71** 2720
[46] Katoh N, Miyazaki T and Ohno T 1999 *Phys. Rev.* B **59** R12723
[47] Galy J 1992 *J. Solid State Chem.* **100** 229
[48] Horsch P and Mack F 1998 *Eur. Phys. J.* B **5** 367
[49] Suaud N and Lepetit M B 2002 *Phys. Rev. Lett.* **88** 056405
[50] Hozoi L, Nishimoto S and Yamasaki A 2005 *Phys. Rev.* B **72** 195117
[51] Hozoi L, de Vries A H, van Oosten A B, Broer R, Cabrero J and de Graaf C 2002 *Phys. Rev. Lett.* **89** 076407
Hozoi L, Presura C, de Graaf C and Broer R 2003 *Phys. Rev.* B **67** 035117
[52] Suaud N and Lepetit M B 2000 *Phys. Rev.* B **62** 402
[53] Popović Z S and Vukajlović F R 1999 *Phys. Rev.* B **59** 5333
[54] Korbel P, Wójcik W, Klejnberg A, Spalek J, Acquarone M and Lavagna M 2003 *Eur. Phys. J.* B **32** 315
[55] Moukouri S and Jarrell M 2001 *Phys. Rev. Lett.* **87** 167010
[56] Slater J C 1951 *Phys. Rev.* **82** 538
[57] Riera J and Poilblanc D 1999 *Phys. Rev.* B **59** 2667